# Photochemical and Photophysical Properties of *fac*-[Re(CO)$_3$(L)$_2$Cl] (L = quinoline or isoquinoline)†

**Neyde Murakami Iha and Guillermo Ferraudi***
*Radiation Laboratory, University of Notre Dame, Notre Dame, IN 46556, USA*

Two new complexes, *fac*-[Re(CO)$_3$(L)$_2$Cl] (L = quinoline or isoquinoline), have been prepared and characterized by X-ray crystallography and spectroscopies. Extended-Hückel molecular orbital calculations were applied to the interpretation UV/VIS spectra of the complexes. Their photochemical and photophysical properties were investigated under steady and flash irradiations. While room-temperature luminescence appears strongly related to the metal-to-ligand charge-transfer excited states, the radiative relaxation of the intraligand excited states dominates the 77 K emissions. The photochemical reactions of *fac*-[Re(CO)$_3$(L)$_2$Cl] (L = quinoline or isoquinoline) are similar to those of *fac*-[Re(CO)$_3$(4Ph-py)$_2$Cl] (4Ph-py = 4-phenylpyridine) and expected to originate in intraligand and/or ligand-to-ligand charge-transfer excited states.

The photochemical and photophysical properties of *cis*-[Re(CO)$_4$(L)X] and *fac*-[Re(CO)$_3$L$_2$X] (X = halide, azine or phosphine; $L_2$ = two monodentate or one bidentate azine) have been the subject of numerous studies.[1–26] Examples in the literature show that the majority of these complexes emit light under irradiation at wavelengths of the first absorption band.[11,14–19,24–26] The origin of such a luminescence, *i.e.* radiative relaxation from either or both metal-to-ligand charge-transfer excited states [m.l.c.t.(azine ⟵ Re)] and intraligand (i.l.) excited states, depends on the azine ligand and on medium conditions.

A number of photoreactions [equations (1) and (2);[6] pip = piperidine] provide alternative ways for the degradation of excess electronic energy. When the Re$^{I}$ complexes were irradiated with photonic energies larger than 390 kJ mol$^{-1}$, various photoredox reactions ensued, equations (3)–(5).[6,24,25]

$$cis\text{-}[Re(CO)_4(PPh_3)I] \xrightarrow[pip]{h\nu} [Re(CO)_3(pip)(PPh_3)I] + CO \quad (1)$$

$$cis\text{-}[Re(CO)_4(PPh_3)I] \xrightarrow[pip]{h\nu} [Re(CO)_4(pip)I] + PPh_3 \quad (2)$$

$$cis\text{-}[Re(CO)_4(PPh_3)I] \xrightarrow[\lambda_{ex} \leqslant 300\ nm]{h\nu} [\{Re(CO)_4(PPh_3)\}_2] + I_2 \quad (3)$$

$$fac\text{-}[Re(CO)_3(4Ph\text{-}py)_2Cl] \xrightarrow[\lambda_{ex} \leqslant 300\ nm]{h\nu} [Re(CO)_3(4Ph\text{-}py^{\bullet+})(4Ph\text{-}py^{\bullet-})Cl] \quad (4)$$

$$fac\text{-}[Re(CO)_3(4Ph\text{-}py)_2Cl] \xrightarrow[\lambda_{ex} \leqslant 300\ nm]{h\nu} [Re(CO)_3(4Ph\text{-}py)Cl]^+ + 4Ph\text{-}py^{\bullet-} \longrightarrow \tfrac{1}{2}[\{Re(CO)(4Ph\text{-}py)(MeCN)_2Cl\}_2] \quad (5)$$

The biradical intermediate, [Re(CO)$_3$(L$^{\bullet+}$)(L$^{\bullet-}$)Cl], has been detected with L = 4-phenylpyridine (4Ph-py) but not with L = 4-cyanopyridine (4CN-py).[24] In this regard, the reaction [equation (4)] is suspected to originate in excited states with intraligand and/or ligand-to-ligand charge-transfer character [l.l.c.t.(azine ⟵ azine)] and close in energy to various m.l.c.t.(azine ⟵ Re) states.[27] Literature reports on the spectroscopy of quinoline (quin) and isoquinoline (iquin) suggest that this condition can also be fulfilled when they or their derivatives are used as azine ligands instead of 4Ph-py.[28–31] In order to demonstrate such a relationship we have prepared the new compounds *fac*-[Re(CO)$_3$(L)$_2$Cl] (L = quin or iquin) and determined their crystal structures. Their photochemical and photophysical properties have been studied and are compared with those of homologous rhenium complexes.

## Experimental

*Materials.*—The complexes *fac*-[Re(CO)$_3$(L)$_2$Cl] (L = quin or iquin) were prepared by modified published procedures.[10,12] Strem or Atomergic [Re(CO)$_5$Cl] and an excess of the ligand L, typically a 1:2.5 mol ratio, were dissolved in benzene (50 cm$^3$) and heated to 60 °C. The solid precipitated from the solution was separated by filtration and washed with benzene. The product was recrystallized five times by the addition of *n*-pentane to its solution in dichloromethane. The purity of the material was ascertained by elemental analysis {Found: C, 44.50; H, 2.45; Cl, 6.60; N, 5.00; O, 8.45. Found: C, 44.10; H, 2.45; Cl, 6.65; N, 4.90; O, 8.60. Calc. for [Re(CO)$_3$(iquin)$_2$Cl]: C, 44.70; H, 2.50; Cl, 6.30; N, 4.95; O, 8.50%}.

Purified [CuL′][ClO$_4$]$_2$ (L′ = 2,3,9,10-tetramethyl-1,4,8,11-tetraazacyclotetradeca-1,3,8,10-tetraene) and [Co(NH$_3$)$_5$Br]-Br$_2$ were available from previous work.[24,25] Quinoline was purified by distillation under vacuum. Aldrich HPLC solvents were used without further purification.

*Determination of Crystal Structures.*—Crystals grown from $CH_2Cl_2$ by slow evaporation were used for the data collection. Measurements, structure solution and data refinement were carried out at the Notre Dame X-Ray Crystallographic Facility.

*Data collection and reduction.* A transparent yellow parallelepiped single crystal of *fac*-[Re(CO)$_3$(iquin)$_2$Cl] of approximate dimensions 0.28 × 0.30 × 0.34 mm was mounted on the end of a hollow glass fibre in a random orientation using cyanoacrylate glue. In a similar procedure, a transparent light yellow crystal cut from a larger plate single crystal of *fac*-

† *Supplementary data available:* see Instructions for Authors, *J. Chem. Soc., Dalton Trans.*, 1994, Issue 1, pp. xxiii–xxviii.

$[Re(CO)_3(quin)_2Cl]$, approximate dimensions 0.30 × 0.43 × 0.45 mm, was mounted with the φ axis approximately perpendicular to the plate face. Preliminary X-ray examination and data collection were performed using Mo-Kα radiation ($\bar{\lambda}$ = 0.710 73 Å) on an Enraf-Nonius CAD4 diffractometer equipped with a graphite crystal incident beam monochromator operating at 294 ± 1 K. Cell constants and an orientation matrix for data collection were obtained from least-squares refinement, based on the setting angles of 25 reflections in the ranges $35.4 < 2\theta < 44.0°$ for the iquin complex and $18.2 < 2\theta < 39.8°$ for the quin. The values were determined by using the computer-controlled diagonal slit method of centring in conjunction with the SET 4 routine.

The data were collected at a temperature of 294 ± 1 K using the θ–2θ scan technique. The scan rate was allowed to vary from 3.30 to 4.12° $min^{-1}$ (in ω). The scan range (in °) was determined as a function of θ to correct for the separation of the Kα doublet. The scan width was estimated to be 0.90 + 0.344 tan θ° and an additional 25% above and below this range were collected to ensure adequate background ranges. Lorentz and polarization corrections were applied. Plots of the intensities of these standard reflections did not show any systematic variation during the time required for the data collection and no correction for decay was applied.

*Structure solution and refinement.* The position of the rhenium atom was determined by the heavy-atom Patterson method. Positions for the other 27 non-hydrogen atoms were found easily from a Fourier difference electron-density map. Positions for the 14 hydrogens atoms were found from a different Fourier electron-density map calculated after preliminary refinement of the non-hydrogen atoms. The structure was refined by full-matrix least squares where the function minimized was $\Sigma w(|F_o| - |F_c|)^2$ and the weight, $w$, is defined $w = 4F_o2\sigma^2(F_o^2) = 1/\sigma^2F_o$. The standard deviation on intensities is defined by $\sigma^2(F_o^2) = [S^2(C + R^2B) + p^2F_o^2]/L_p^2$, where $S$ is the scan rate, $C$ the total integrated peak count, $R$ the ratio of scan time to background counting time, $B$ the total background count, $L_p$ the Lorentz-polarization factor, and the parameter $p$ (here set to 0.02) a factor introduced to downweight intense reflections.

Scattering factors were taken from Cromer and Weber.[32–34] The model for the final cycles of refinement assigned the anisotropic thermal parameters to the non-hydrogen atoms. It also included the H-atom coordinates and isotropic thermal parameters as fixed parameters [initially idealized with $d$(C–H) 0.98 Å and $B$(H) = 1.2 $B$ with attached carbon]. All calculations were performed on a VAX station 3200 using the SDP/VAX program system.[35,36]

Additional material available from the Cambridge Crystallographic Data Centre comprises H-atom coordinates and thermal parameters.

*Vibrational Spectroscopy.*—The IR spectra were recorded on a Perkin-Elmer 783 spectrophotometer in KBr pellets. Raman spectra were collected on a Jarrel Ash apparatus with a double monochromator (4 $cm^{-1}$ spectral resolution). Light of wavelength 647.1 nm from a krypton-ion laser was used for the excitation. Spectra were obtained from powder samples placed on a rotatory Nylon disk.

*Theoretical Calculations.*—Semiempirical calculations were carried in the manner described elsewhere.[37] Extended-Hückel molecular orbital (MO) calculations were carried out with a modified Forticon program, QCPE Program No. 344. Contour plots of the point probability, $|\psi|^2$, were calculated for several contour levels of a molecular orbital, ψ. The molecular orbitals were expressed as polynomials where each term was a product of a given Slater-type atomic orbital and the corresponding coefficient in the output of Forticon.

*Flash Photochemical Procedures.*—The flash photolysis apparatus for the study of reaction kinetics and the measurement of transient absorption or emission spectra in a picosecond to second time domain have been described elsewhere.[38,39] In these experiments, 10 ns flashes of monochromatic light were respectively generated with a Nd:YAG (Quanta Ray), an excimer (Lambda Physik), or a $N_2$ laser (Laser Photonics, PRA/model UV-24). The calculation of the number of photons absorbed by the photolyte was based on actinometry with $[Co(NH_3)_5Br]^{2+}$.[24,25] Irradiation of the $Co^{III}$ complex in an aqueous acidic (pH 3) solution of NaBr generated $Br_2^-$ whose concentration, $[Br_2^-]_0$, was determined from the spectral change measured 0.2 μs after the flash. Literature values of the absorption coefficients for $Br_2^-$ and quantum yields for the generation of the radical ion were used for the calculation.[24,25] Concentrations of the $Co^{III}$ complex were selected under the condition that solutions of the actinometer and a given photolyte have the same absorbance at the wavelength, $\lambda_{ex}$, chosen for the irradiation. Solutions were deaerated with oxygen-free nitrogen in a gas-tight apparatus. In the reaction cell the liquid was refreshed after each irradiation. A mode-locked Nd:YAG laser was used as a source of pulses of 355 or 266 nm light with a 18 ps width for flash photochemical experiments in a time domain of picoseconds.

*Steady-state Irradiations.*—Steady-state 254 nm photolyses were carried out in an irradiator with a low-pressure mercury lamp (Rayonet). The concentrations of the photolytes were adjusted for absorbing more than 99.99% of the incident light and magnetic bars were used for stirring the solutions while they were irradiated.

The luminescence of the $Re^I$ complexes was investigated using an SLM-Aminco 8000C spectrofluorometer with instrument response corrections.

Streams of oxygen-free nitrogen were used to deaerate the solutions used in the photochemical and photophysical experiments.

## Results

*Molecular Structure.*—The molecular structures of *fac*-$[Re(CO)_3(L)_2Cl]$ (L = quin or iquin) are shown in Fig. 1. Crystallographic data are given in Table 1 and geometrical parameters in Tables 2 and 3. The structures reveal significant departures of some angles about rhenium from 90°. Molecular planes of the azine ligands, quin and iquin, form near 45° dihedral angles with the corresponding co-ordinate planes. In the iquin complex the rhenium–ligand bond distances are very close to literature values for other *fac*-$[Re(CO)_3(azine)_2Cl]$ complexes.[40] The Re–N(1) and Re–N(2) bond distances in *fac*-$[Re(CO)_3(quin)_2Cl]$ are longer than those measured in the iquin analogue. Such a difference can be correlated with a stronger Re–iquin bond and to the greater σ-donating character of iquin relative to quin.[41] These relationships between bond length and bond strength were also reflected in the metal and ligand vibrations.*

*MO Calculations and Absorption Spectra.*—Extended-Hückel MO calculations were carried out with bond distances and angles extracted from the X-ray measurements. In *fac*-$[Re(CO)_3(quin)_2Cl]$ and *fac*-$[Re(CO)_3(iquin)_2Cl]$ the highest occupied molecular orbital (HOMO) is mainly a rhenium-centred orbital, Fig. 2(*a*). Several unoccupied MO orbitals, some formed with orbitals of the azine ligands, appear above the HOMO at energies of the first absorption band, Fig. 2(*b*). The assignment of the orbitals was tested by modelling the

* Vibrations with frequencies 410, 495 and 510 $cm^{-1}$ (probably Re–CO and Re–Cl vibrations)[42] in the spectrum of the quin complex appear at 380, 470 and 480 $cm^{-1}$ in the spectrum of the iquin complex. By contrast, the asymmetric deformation of the azine was placed at 766–630 $cm^{-1}$ in the former and at 818–778 $cm^{-1}$ in the latter.

**Table 1** Crystal data and intensity data collection parameters

| Compound | $[Re(CO)_3(iquin)_2Cl]$ | $[Re(CO)_3(quin)_2Cl]$ |
|---|---|---|
| Empirical formula | $C_{21}H_{14}ClN_2O_3Re$ | $C_{21}H_{14}ClN_2O_3Re$ |
| $M$ | 564.01 | 564.01 |
| Crystal dimensions/mm | 0.28 × 0.30 × 0.34 | 0.30 × 0.43 × 0.45 |
| $T$/K | 294 ± 1 | 294 ± 1 |
| Crystal system | Monoclinic | Monoclinic |
| Space group | $P2_1/n$ (no. 14) | $P2_1/n$ (no. 14) |
| $a$/Å | 10.239(1) | 9.431(1) |
| $b$/Å | 15.659(2) | 15.596(2) |
| $c$/Å | 13.096(1) | 13.229(1) |
| β/° | 110.77(1) | 91.79(1) |
| $U$/Å$^3$ | 1963.4(6) | 1945.0(6) |
| $Z$ | 4 | 4 |
| $D_c$/g cm$^{-3}$ | 1.91 | 1.93 |
| μ(Mo-Kα)/cm$^{-1}$ | 64.3 | 64.9 |
| Scan type | θ–2θ | θ–2θ |
| 2θ range/° | 3.0–58.70 | 3.0–58.70 |
| sinθ/λ maximum | 0.689 | 0.689 |
| Total data measured | 11 077 | 11 058 |
| Unique measured | 5375 | 5319 |
| Unique $F_o > 3\sigma(F_o)$ | 4579 | 4300 |
| Data : variable ratio | 18.1 | 17.0 |
| $R$ | 0.022 | 0.029 |
| $R'$ | 0.024 | 0.033 |
| Goodness of fit | 1.14 | 1.53 |
| Convergence, largest shift/error | 0.10 | 0.01 |
| Highest peak in final difference map/e Å$^{-3}$ | 0.58(10) | 2.46(8) (near Re)<br>0.47 (not near Re) |

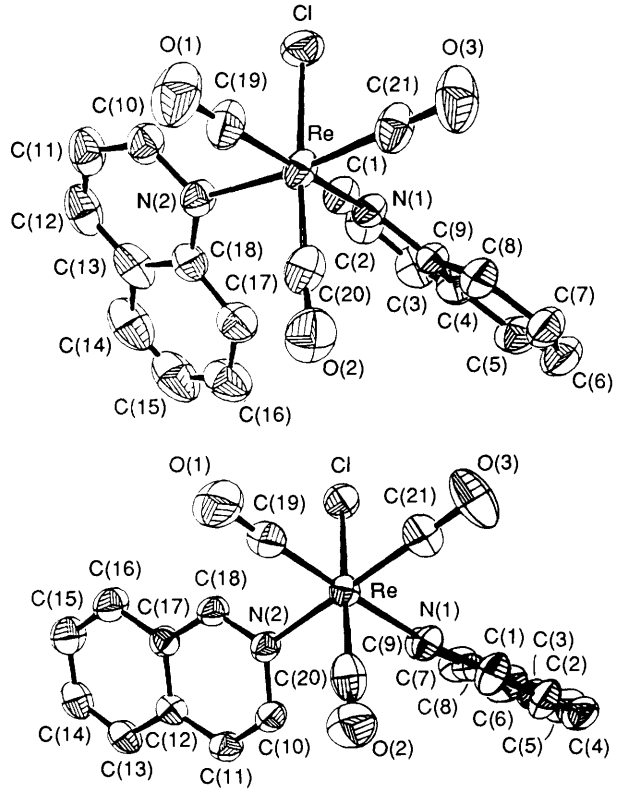


**Fig. 1** Molecular structures of (*a*) *fac*-$[Re(CO)_3(quin)_2Cl]$ and (*b*) *fac*-$[Re(CO)_3(iquin)_2Cl]$, showing the atom numbering scheme. Thermal ellipsoids are drawn at the 50% probability level. Hydrogen atoms are omitted for clarity

absorption spectra of the rhenium complexes, Fig. 3. In order to do this relevant electronic transitions were represented by Gaussian functions. Oscillator strengths (width and maximum intensity) for each particular function were assigned from the

**Table 2** Interatomic bond distances (Å) with estimated standard deviations (e.s.d.s) in the least significant figure given in parentheses

(*a*) *fac*-$[Re(CO)_3(iquin)_2Cl]$

| | | | |
|---|---|---|---|
| Re–Cl | 2.4686(8) | C(3)–C(8) | 1.420(4) |
| Re–N(1) | 2.204(3) | C(4)–C(5) | 1.344(6) |
| Re–N(2) | 2.207(2) | C(5)–C(6) | 1.407(6) |
| Re–C(19) | 1.909(4) | C(6)–C(7) | 1.355(5) |
| Re–C(20) | 1.969(4) | C(7)–C(8) | 1.409(4) |
| Re–C(21) | 1.896(3) | C(8)–C(9) | 1.406(4) |
| O(1)–C(19) | 1.142(4) | C(10)–C(11) | 1.350(4) |
| O(2)–C(20) | 1.029(4) | C(11)–C(12) | 1.407(4) |
| O(3)–C(21) | 1.153(4) | C(12)–C(13) | 1.419(4) |
| N(1)–C(1) | 1.379(4) | C(12)–C(17) | 1.413(4) |
| N(1)–C(9) | 1.315(4) | C(13)–C(14) | 1.361(5) |
| N(2)–C(10) | 1.372(4) | C(14)–C(15) | 1.395(5) |
| N(2)–C(18) | 1.320(3) | C(15)–C(16) | 1.373(4) |
| C(1)–C(2) | 1.352(4) | C(16)–C(17) | 1.413(4) |
| C(2)–C(3) | 1.393(5) | C(17)–C(18) | 1.405(4) |
| C(3)–C(4) | 1.410(5) | | |

(*b*) *fac*-$[Re(CO)_3(quin)_2Cl]$

| | | | |
|---|---|---|---|
| Re–Cl | 2.474(1) | C(4)–C(5) | 1.403(5) |
| Re–N(1) | 2.247(2) | C(4)–C(9) | 1.407(4) |
| Re–N(2) | 2.264(3) | C(5)–C(6) | 1.339(6) |
| Re–C(19) | 1.903(4) | C(6)–C(7) | 1.407(6) |
| Re–C(20) | 1.890(4) | C(7)–C(8) | 1.356(4) |
| Re–C(21) | 1.894(3) | C(8)–C(9) | 1.413(4) |
| O(1)–C(19) | 1.147(4) | C(10)–C(11) | 1.398(5) |
| O(2)–C(20) | 1.143(5) | C(11)–C(12) | 1.333(6) |
| O(3)–C(21) | 1.150(4) | C(12)–C(13) | 1.424(7) |
| N(1)–C(1) | 1.318(4) | C(13)–C(14) | 1.413(6) |
| N(1)–C(9) | 1.390(4) | C(13)–C(18) | 1.396(5) |
| N(2)–C(10) | 1.328(4) | C(14)–C(15) | 1.332(8) |
| N(2)–C(18) | 1.398(4) | C(15)–C(16) | 1.401(7) |
| C(1)–C(2) | 1.395(5) | C(16)–C(17) | 1.381(6) |
| C(2)–C(3) | 1.334(6) | C(17)–C(18) | 1.403(5) |
| C(3)–C(4) | 1.428(6) | | |

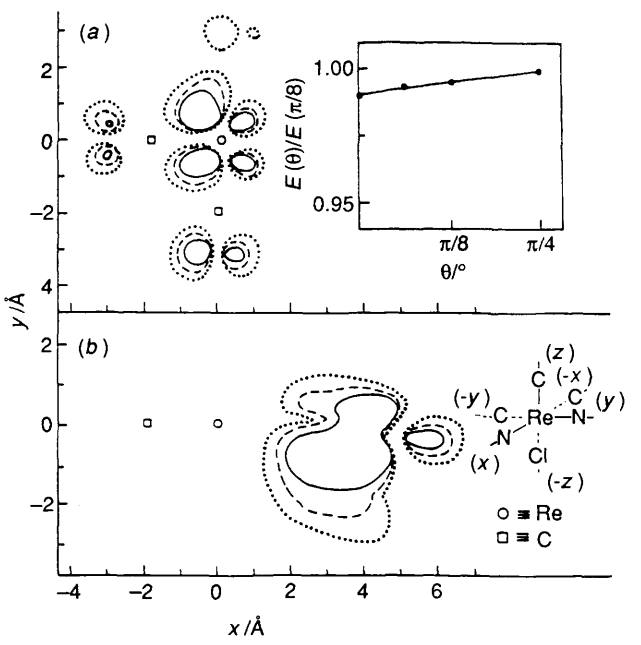


**Fig. 2** Plots of the contour curves for the point probability, $|\psi|^2$, of the HOMO (*a*) and LUMO (*b*) in *fac*-$[Re(CO)_3(iquin)_2Cl]$. The positions of various atoms in the first co-ordination sphere and the key to atoms intercepted by the *xy* coordinate planes are shown in (*b*). The insert to (*a*) shows the dependence of the ground-state electronic energy on the dihedral angle, θ, between a given coordinate plane and the molecular plane of the iquin ligand

literature.[43,44] The distribution of electronic levels found in the calculations indicates the proximity in energy of two manifolds

**Table 3** Interatomic bond angles (°) with e.s.d.s in parentheses

(*a*) *fac*-[Re(CO)$_3$(iquin)$_2$Cl]

| | | | |
|---|---|---|---|
| C(1)–Re–N(1) | 86.45(7) | C(1)–C(2)–C(3) | 121.2(3) |
| C(1)–Re–N(2) | 85.60(6) | C(2)–C(3)–C(4) | 124.7(3) |
| Cl–Re–C(19) | 91.98(9) | C(2)–C(3)–C(8) | 116.8(3) |
| Cl–Re–C(20) | 176.2(1) | C(4)–C(3)–C(8) | 118.5(3) |
| Cl–Re–C(21) | 91.1(1) | C(3)–C(4)–C(5) | 120.4(3) |
| N(1)–Re–N(2) | 86.05(9) | C(4)–C(5)–C(6) | 121.1(3) |
| N(1)–Re–C(19) | 178.4(1) | C(5)–C(6)–C(7) | 120.5(4) |
| N(1)–Re–C(20) | 90.5(1) | C(6)–C(7)–C(8) | 119.8(3) |
| N(1)–Re–C(21) | 92.5(1) | C(3)–C(8)–C(7) | 119.6(3) |
| N(2)–Re–C(19) | 93.5(1) | C(3)–C(8)–C(9) | 118.1(3) |
| N(2)–Re–C(20) | 91.9(1) | C(7)–C(8)–C(9) | 122.2(3) |
| N(2)–Re–C(21) | 176.5(1) | N(1)–C(9)–C(8) | 123.8(3) |
| C(19)–Re–C(20) | 91.0(1) | N(2)–C(10)–C(11) | 123.0(3) |
| C(19)–Re–C(21) | 87.9(1) | C(10)–C(11)–C(12) | 120.3(3) |
| C(20)–Re–C(21) | 91.3(1) | C(11)–C(12)–C(13) | 124.6(3) |
| Re–C(19)–O(1) | 178.4(3) | C(11)–C(12)–C(17) | 117.2(2) |
| Re–C(20)–O(2) | 177.7(3) | C(13)–C(12)–C(17) | 118.2(3) |
| Re–C(21)–O(3) | 178.9(3) | C(12)–C(13)–C(14) | 120.2(3) |
| Re–N(1)–C(1) | 119.1(2) | C(13)–C(14)–C(15) | 121.5(3) |
| Re–N(1)–C(9) | 123.2(2) | C(14)–C(15)–C(16) | 120.3(3) |
| C(1)–N(1)–C(9) | 117.5(3) | C(15)–C(16)–C(17) | 119.5(3) |
| Re–N(2)–C(10) | 121.8(2) | C(12)–C(17)–C(16) | 120.4(3) |
| Re–N(2)–C(18) | 120.6(2) | C(12)–C(17)–C(18) | 118.2(3) |
| C(10)–N(2)–C(18) | 117.6(2) | C(16)–C(17)–C(18) | 121.5(3) |
| N(1)–C(1)–C(2) | 112.4(3) | N(2)–C(18)–C(17) | 123.7(3) |

(*b*) *fac*-[Re(CO)$_3$(quin)$_2$Cl]

| | | | |
|---|---|---|---|
| Cl–Re–N(1) | 84.13(7) | C(1)–C(2)–C(3) | 120.0(4) |
| Cl–Re–N(2) | 86.41(8) | C(2)–C(3)–C(4) | 118.7(3) |
| Cl–Re–C(19) | 93.4(1) | C(3)–C(4)–C(5) | 121.9(3) |
| Cl–Re–C(20) | 177.2(1) | C(3)–C(4)–C(9) | 118.8(3) |
| Cl–Re–C(21) | 87.7(1) | C(5)–C(4)–C(9) | 119.3(3) |
| N(1)–Re–N(2) | 85.8(1) | C(4)–C(5)–C(6) | 121.7(4) |
| N(1)–Re–C(19) | 175.4(1) | C(5)–C(6)–C(7) | 119.1(3) |
| N(1)–Re–C(20) | 94.4(1) | C(6)–C(7)–C(8) | 121.5(3) |
| N(1)–Re–C(21) | 95.9(1) | C(7)–C(8)–C(9) | 120.0(3) |
| N(2)–Re–C(19) | 90.1(1) | N(1)–C(9)–C(4) | 120.6(3) |
| N(2)–Re–C(20) | 95.8(1) | N(1)–C(9)–C(8) | 121.1(3) |
| N(2)–Re–C(21) | 173.7(1) | C(4)–C(9)–C(8) | 118.4(3) |
| C(19)–Re–C(20) | 88.2(2) | N(2)–C(10)–C(11) | 123.8(4) |
| C(19)–Re–C(21) | 88.0(1) | C(10)–C(11)–C(12) | 119.7(4) |
| C(20)–Re–C(21) | 90.1(2) | C(11)–C(12)–C(13) | 119.4(4) |
| Re–C(19)–O(1) | 179.4(4) | C(12)–C(13)–C(14) | 121.8(4) |
| Re–C(20)–O(2) | 177.3(3) | C(12)–C(13)–C(18) | 118.6(4) |
| Re–C(21)–O(3) | 178.3(3) | C(14)–C(13)–C(18) | 119.6(5) |
| Re–N(1)–C(1) | 116.4(2) | C(13)–C(14)–C(15) | 120.4(5) |
| Re–N(1)–C(9) | 125.2(2) | C(14)–C(15)–C(16) | 120.9(4) |
| C(1)–N(1)–C(9) | 117.7(3) | C(15)–C(16)–C(17) | 120.2(5) |
| Re–N(2)–C(10) | 115.7(2) | C(16)–C(17)–C(18) | 119.5(4) |
| Re–N(2)–C(18) | 126.9(2) | N(2)–C(18)–C(13) | 120.9(4) |
| C(10)–N(2)–C(18) | 117.3(3) | N(2)–C(18)–C(17) | 119.8(3) |
| N(1)–C(1)–C(2) | 124.1(3) | C(13)–C(18)–C(17) | 119.3(4) |

of electronic states: one level with m.l.c.t.(azine ← Re) character and another of intraligand states with $\pi\pi^*$ character.

*Photophysical Properties.*—Broad unstructured emission spectra were recorded when deaerated solutions of *fac*-[Re(CO)$_3$(L)$_2$Cl] (L = quin or iquin) were irradiated between 330 and 360 nm, Fig. 4(*a*). The excitation spectra, Fig. 4(*b*), relate such emissions to irradiation of the rhenium complexes at wavelengths of the first intense band in the absorption spectra. The same lifetimes were recorded for the decay of the emissions and for transient absorption spectra in flash photolyses, Fig. 5. Since the decay of the absorbance within several microseconds leaves almost no residual absorption indicative of photoproducts, the spectra in Fig. 5 can be assigned to excited states undergoing radiative and radiationless relaxations. It must be noted, however, that some photoreactions with very low quantum yields (below) were detected for laser irradiation at wavelengths between 330 and 360 nm.

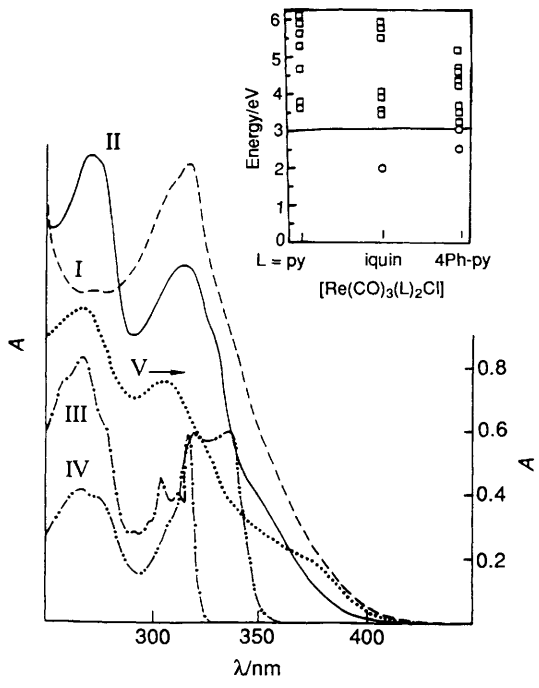


**Fig. 3** Absorption spectra of *fac*-[Re(CO)$_3$(quin)$_2$Cl] in $CH_2Cl_2$ (I, $\lambda_{max}$ 315 nm, $\varepsilon_{max}$ 1.2 × $10^4$ dm$^3$ mol$^{-1}$ cm$^{-1}$), *fac*-[Re(CO)$_3$(iquin)$_2$Cl] in MeCN (II, $\lambda_{max}$ 308, 268 nm, $\varepsilon_{max}$ 1.5 × $10^4$, 2.2 × $10^4$ dm$^3$ mol$^{-1}$ cm$^{-1}$), iquin [28–31] in MeCN (III) and Hiquin·ClO$_4$ [28–31] in ethanol (IV). Curve V is a typical output after modelling the spectrum of *fac*-[Re(CO)$_3$(iquin)$_2$Cl] with electronic levels in the insert. The insert shows the unoccupied electronic levels above the HOMO for various Re$^I$ complexes (py = pyridine): ○, ligand centred and □, mixed rhenium–ligand character. The vertical scales are arbitrary for the sake of comparisons between various spectra

In 355 nm flash photolysis of the iquin complex, the appearance of the spectrum in Fig. 5 is nearly 80% complete in less than 30 ps, *i.e.* the time resolution of the instrument. The final 20% of the absorbance grows exponentially with a (3.0 ± 0.9) × $10^2$ ps lifetime.

The low-temperature, *i.e.* 77 K, emission of the complexes in diethyl ether–isopentane–ethanol (5:5:2) or ethanol is more structured, Fig. 6(*a*), and similar to literature spectra for the phosphorescence of the protonated azines.[28–31] In ethanol at 77 K the decay of the emission is described by a double exponential with lifetimes $\tau_1$ and $\tau_2$. The fast component of the decay has nanosecond lifetimes, *i.e.* $\tau_1$ = 10 ± 2 ns for *fac*-[Re(CO)$_3$(iquin)$_2$Cl] and $\tau_1$ = 16 ± 3 ns for *fac*-[Re(CO)$^3$-(quin)$_2$Cl]. The slow component has lifetimes of several hundred microseconds, *i.e.* $\tau_2$ = 340 ± 20 μs for [Re(CO)$_3$-(iquin)$_2$Cl] and $\tau_2$ = 250 ± 70 μs for *fac*-[Re(CO)$_3$(quin)$_2$Cl].

Vibronic components were well resolved for the 77 K emission of *fac*-[Re(CO)$_3$(iquin)$_2$Cl] doped in [Re(CO)$_5$Cl], Fig. 6(*b*). The time-resolved decay of such an emission, like those in glassy solutions, could also be fitted to a double exponential with $\tau_1$ = 72 ± 5 ns and $\tau_2$ = 160 ± 20 ns.

*Photoreactions.*—Photochemical reactions were investigated by laser flash irradiation of 3.0 × $10^{-4}$–1.0 × $10^{-4}$ mol dm$^{-3}$ *fac*-[Re(CO)$_3$(quin)$_2$Cl] in $CH_2Cl_2$ or *fac*-[Re(CO)$_3$(iquin)$_2$Cl] in MeCN at wavelengths of the first absorption band, $\lambda_{ex}$ > 308 nm. Small spectral changes, observed more than 2 μs after the flash, were indicative of poor conversion to photoproducts. The primary photoreactions, $\lambda_{ex}$ ⩽ 308 nm, of *fac*-[Re(CO)$_3$-(iquin)$_2$Cl] in MeCN were found to be similar to those of *fac*-[Re(CO)$_3$(4Ph-py)$_2$Cl], equations (4) and (5). Intermediates with a biradical nature were investigated *via* flash irradiation of *fac*-[Re(CO)$_3$(iquin)$_2$Cl] in solutions 1 × $10^{-5}$–3.0 × $10^{-4}$ mol dm$^{-3}$ in [CuL′]$^{2+}$. Time-resolved measurements of the

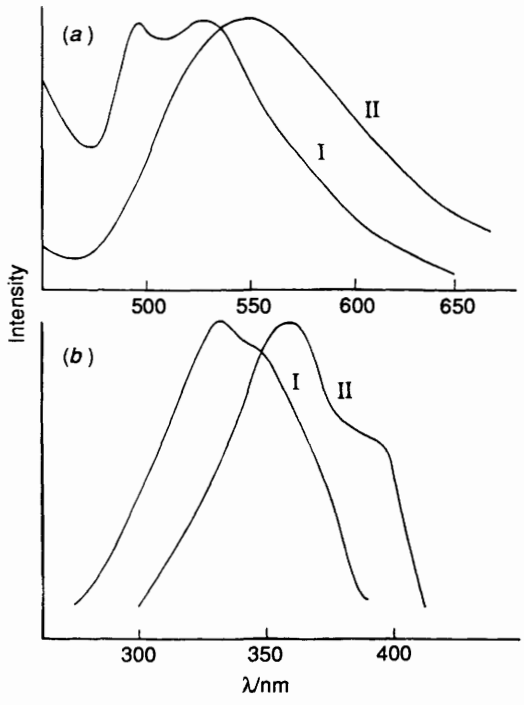


**Fig. 4** Room-temperature emission spectra (*a*) measured with deaerated solutions of *fac*-$[Re(CO)_3(iquin)_2Cl]$ in MeCN (I, $\lambda_{ex}$ 330 nm) and *fac*-$[Re(CO)_3(quin)_2Cl]$ in $CH_2Cl_2$ (II, $\lambda_{ex}$ 360 nm). The corresponding excitation spectra, shown in (*b*), were determined with I, $\lambda_{em}$ 525 nm and II, $\lambda_{em}$ 550 nm

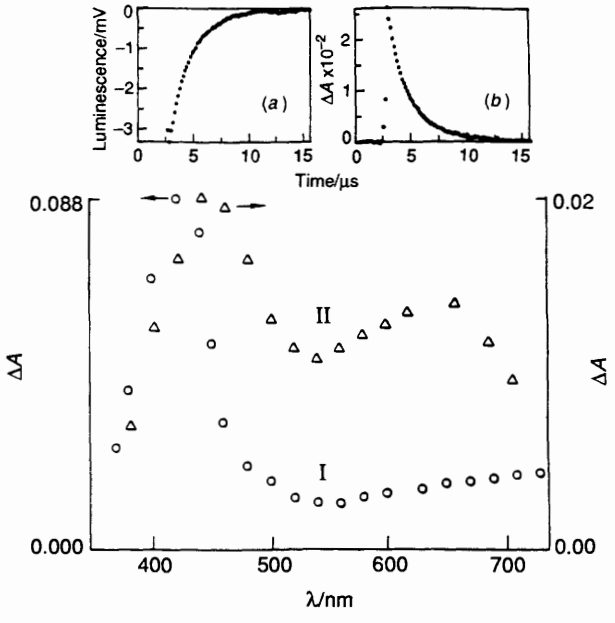


**Fig. 5** Transient spectra recorded 300 ns after the flash irradiation of deaerated $10^{-4}$ mol $dm^{-3}$ *fac*-$[Re(CO)_3(iquin)_2Cl]$ in MeCN (I, $\lambda_{ex}$ 308 nm) and $1.8 \times 10^{-4}$ mol $dm^{-3}$ *fac*-$[Re(CO)_3(quin)_2Cl]$ in $CH_2Cl_2$ (II, $\lambda_{ex}$ 337 nm). The inserts show traces for the time-resolved decay of the 550 nm emission (*a*) and the decay of the 460 nm absorbance on flash irradiation of *fac*-$[Re(CO)_3(quin)_2Cl]$

absorbance and luminescence intensity revealed the formation of $[CuL']^+$, $\lambda_{max} \approx 745$ nm, with a parallel quenching of the emission, Table 4.[19,24] This method for detecting the biradical intermediate has been applied previously to the photochemical reaction $[Re(CO)_3(4Ph\text{-}py)_2Cl]$ and $[Re(CO)_3(4CN\text{-}py)_2Cl]$.[19,24] Complete scavenging of the biradical intermediate was accomplished with concentrations of $[CuL']^{2+}$ equal to or

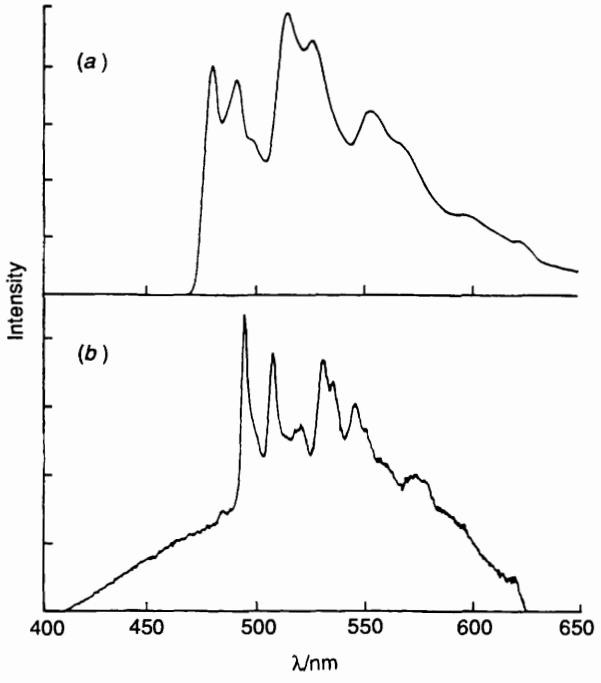


**Fig. 6** Low-temperature (77 K) emission spectra of *fac*-$[Re(CO)_3(iquin)_2Cl]$ in (*a*) glassy methanol solution and (*b*) doped in $[Re(CO)_5Cl]$

greater than $1 \times 10^{-5}$ mol $dm^{-3}$. These results show that the reaction between $[CuL']^{2+}$ and the biradical intermediate was very fast, *i.e.* near diffusion controlled with $k \approx 10^{10}$ $dm^3$ $mol^{-1}$ $s^{-1}$. By contrast, the dependence of the luminescence lifetime on the concentration of $[CuL']^{2+}$ resulted in a rate constant, $k_q \approx 2.6 \times 10^9$ $dm^3$ $mol^{-1}$ $s^{-1}$, for the quenching reaction. A biradical intermediate was also detected in the flash photolysis of *fac*-$[Re(CO)_3(quin)_2Cl]$ by reaction with $[CuL']^{2+}$.

Spectral changes, Fig. 7, in continuous and flash photolyses with $\lambda_{ex} \leqslant 308$ nm were similar to those previously reported for the $Re^I$ dimer photoproduct from photolysis of *fac*-$[Re(CO)_3(4Ph\text{-}py)_2Cl]$, equation (5).[24] Typical spectral changes are, for example, a new absorption band between 400 and 450 nm that grows with the irradiation. In accordance with these experimental observations, optical transients in a microsecond time domain, insert to Fig. 7, can be assigned to intermediates, *i.e.* short-lived $Re^{II}$ species and the corresponding $quin^{\bullet -}$ and $iquin^{\bullet -}$ radicals, in the formation of dimeric $Re^I$ complexes. Appropriate substitutions of 4Ph-py, $4Ph\text{-}py^{\bullet -}$ by iquin, $iquin^{\bullet -}$, or quin, $quin^{\bullet -}$ in equation (5) describe the photochemical processes that $[Re(CO)_3(iquin)_2Cl]$ and $[Re(CO)_3(quin)_2Cl]$ undergo.

## Discussion

The crystal structures of *fac*-$[Re(CO)_3(quin)_2Cl]$ and *fac*-$[Re(CO)_3(iquin)_2Cl]$ are considerably distorted from octahedral geometry. Departures of the co-ordination angles from 90° are appreciable. The molecular planes of quin and iquin form near 45° dihedral angles with the co-ordination planes. The MO calculations show that such geometries minimize repulsive interactions between π-filled orbitals centred in these azine ligands and in $Re^I$. This point is illustrated, Fig. 2, from the electronic energies calculated as a function of the dihedral angle. Indeed, the insert in Fig. 2 shows that maximum stability results at a dihedral angle of 45°. When the empirical nuclear configurations are used in the MO calculations, the end result is a good simulation of the absorption spectra, Fig. 3. In the energy level diagram, insert to Fig. 3, a number of filled and empty molecular orbitals centred on the azine ligands are separated by energies corresponding to the absorptions in the

**Table 4** Quantum yields of $[CuL']^+$ ($\varphi$) from interception of a biradical intermediate and emission lifetimes ($\tau$) in flash photolysis of *fac*-$[Re(CO)_3(iquin)_2Cl]$

| $\lambda_{ex}$/nm | $\varphi^a$ | $\tau^b$/μs |
|---|---|---|
| 354 | 0.014 ± 0.002 | 0.87 ± 0.05 |
| 337 | 0.018 ± 0.005 | 0.94 ± 0.07 |
| 308 | 0.020 ± 0.002 | 0.95 ± 0.05 |
| 266 | 0.023 ± 0.003 | 0.80 ± 0.08 |
| 248 | 0.039 ± 0.008 | 0.90 ± 0.07 |

[a] Measurements carried out with given concentrations of photolyte, $6 \times 10^{-5} \leqslant [fac\text{-}Re(CO)_3(iquin)_2Cl] \leqslant 3 \times 10^{-4}$ mol dm$^{-3}$, as a function of the $Cu^{II}$ complex concentration, *i.e.* $1.0 \times 10^{-5} \leqslant [CuL'^{2+}] \leqslant 3.0 \times 10^{-4}$ mol dm$^{-3}$. [b] Excited-state lifetimes measured in the absence of $[CuL']^{2+}$.

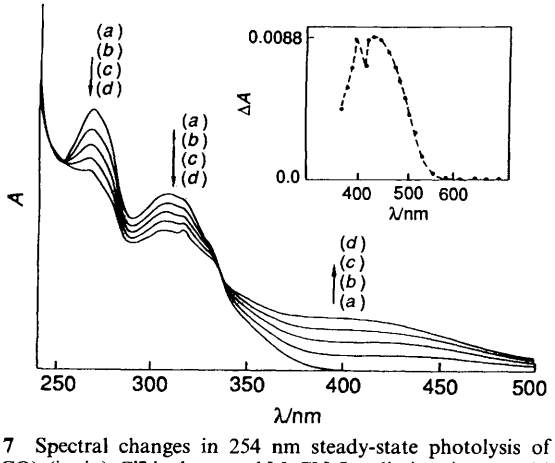


**Fig. 7** Spectral changes in 254 nm steady-state photolysis of *fac*-$[Re(CO)_3(iquin)_2Cl]$ in deaerated MeCN. Irradiation times are (*a*) 100, (*b*) 800, (*c*) 1300, (*d*) 2000 and (*e*) 3300 s. The insert shows the spectrum, recorded 7 μs after the 266 nm flash irradiation of the complex, assigned to a $Re^{II}$ intermediate (see text)

UV spectra of the quin and iquin complexes. A consequence of this array of electronic levels is that the intraligand ππ* (azine-centred) excited states must be close in energy to the lower m.l.c.t.(azine ⟵ Re) states. This vicinity of ππ* and m.l.c.t.-(azine ⟵ Re) states must determine the photochemical and photophysical properties of the rhenium complexes. No such a role is played by the l.l.c.t. states of these complexes according to the experimental observations. In MO calculations where interactions with the medium are ignored, similar energies are calculated for the ππ* and l.l.c.t. states. Indeed, π and π* orbitals of the intraligand state are located in the same azine ligand, *i.e.* they are the HOMO and LUMO in one of the two azine ligands in $[Re(CO)_3(azine)_2Cl]$. In the l.l.c.t. state, charge has been transferred from the π HOMO localized in one azine ligand to a π* LUMO localized in the other azine ligand. Such an electronic transition causes charge separation and the l.l.c.t. state is characterized by a permanent dipole moment. When solvent repolarization is considered, the energy of the l.l.c.t. state is augmented compared to the related ππ* by an amount equal to the work required electrically to charge the l.l.c.t. molecular dipole in the dielectric medium.

Further evidence about the vicinity of the m.l.c.t.(azine ⟵ Re) and intraligand states is provided by the emission spectra of the complexes. The emission spectra and lifetimes of the emission at room temperature are consistent with large contributions from the radiative relaxation of the m.l.c.t.(azine ⟵ Re) state to the luminescence of the complexes.[1-15,24] By contrast, the low-temperature (77 K) emission spectra of *fac*-$[Re(CO)_3(quin)_2Cl]$ and *fac*-$[Re(CO)_3(iquin)_2Cl]$ and the lifetime of the long-lived emission compare very well with the reported phosphorescence of quin and iquin in various media.[30-33] Similarities between the phosphoresence spectra of co-ordinated and protonated ligands indicate that the rhenium centre exerts a perturbation of the intraligand excited states, *i.e.* $^3\pi\pi^*$, which is qualitatively similar to that of the proton. This implies that the overlap between metal d(π) and azine electronic clouds with π symmetries is poor in the ground and excited states.

When the temperature is increased to 298 K, the lifetime of the emission decreases to less than a microsecond and the sharpness of the vibronic structure is diminished. This dependence of the emission on temperature has previously been associated with contributions to the luminescence from the radiative relaxation of the $^3$m.l.c.t.(azine ⟵ Re) states.[1,3,11] It is possible, therefore, that the biphasic decay of the luminescence at 77 K is caused by conversion of the $^3$m.l.c.t.(azine ⟵ Re) state to the emissive $^3\pi\pi^*$ state probably in competition with radiative and radiationless relaxations to the ground state, equations (6)–(8). In the decay

$$^3\text{m.l.c.t.(azine} \longleftarrow \text{Re)} \longrightarrow {}^3\pi\pi^* \quad (6)$$

$$^3\text{m.l.c.t.(azine} \longleftarrow \text{Re)} \longrightarrow fac\text{-}[Re(CO)_3(L)_2Cl] + h\nu \quad (7)$$

$$^3\text{m.l.c.t.(azine} \longleftarrow \text{Re)} \longrightarrow fac\text{-}[Re(CO)_3(L)_2Cl] + \text{heat} \quad (8)$$

$$^3\pi\pi^* \longrightarrow fac\text{-}[Re(CO)_3(L)_2Cl] + h\nu \quad (9)$$

$$^3\pi\pi^* \longrightarrow fac\text{-}[Re(CO)_3(L)_2Cl] + \text{heat} \quad (10)$$

of the emission, this step (lifetime $\tau_1$) must be followed by a slower relaxation of the ππ* state, equations (9) and (10) with a lifetime $\tau_2$.[3]

The mechanism, equations (6)–(10), is similar to one proposed for rhenium complexes of 4-styrylpyridine.[3] The biphasic kinetics can be rationalized whether equation (6) represents thermal equilibration between the l.l.c.t. and ππ* states or the irreversible conversion of the ππ* to the l.l.c.t. It must be noted, however, that a parallel decay of the simultaneously populated m.l.c.t. and ππ* states is another possible mechanism of the luminescence kinetics. In this case the emission spectra of the complexes must be composed of contributions from each excited state.

The excitation spectra show that room-temperature emissions are mainly associated with irradiation within the first absorption band. Photoreactions induced by irradiation at other spectral regions, *i.e.* $\lambda_{ex} \leqslant 308$ nm, provide paths for the degradation of electronic energy. Irradiation at wavelengths shorter than the first absorption band, namely where the population of intraligand states is optically important, photogenerates a biradical intermediate, equation (11),

$$fac\text{-}[Re(CO)_3(L)_2Cl] \xrightarrow[\lambda_{ex} \leqslant 300\text{ nm}]{h\nu} [Re(CO)_3(L^{\bullet+})(L^{\bullet-})Cl] \quad (11)$$

analogous to that generated in the photolysis of *fac*-$[Re(CO)_3(4Ph\text{-}py)_2Cl]$, equation (5).[19,24] The trapping of the biradical by $[CuL']^{2+}$, equation (12), proved to be very fast.

$$[Re(CO)_3(L^{\bullet+})(L^{\bullet-})Cl] + [CuL']^{2+} \longrightarrow [Re(CO)_3(L)(L^{\bullet+})Cl] + [CuL']^+ \quad (12)$$

Quantum yields for the photogeneration of the biradical and the excitation spectrum of the phosphorescence show that the primary process, equation (11), gains significance after the demise of the luminescence. In the photolysis of *fac*-$[Re(CO)_3(L)_2Cl]$ (L = quin or iquin) a narrow range of photonic energies allows the population of the intraligand excited states leading to the biradical intermediate. In this regard the spectral and photochemical properties of the quin and iquin complexes show greater resemblance to those of the 4Ph-py than those of the pyridine (py) or 4CN-py complexes.

**Acknowledgements**

This work was supported by the Office of Basic Energy Sciences of the U.S. Department of Energy. Also acknowledged is a fellowship to N. M. from Fundacao de Amparo a Pesquisa do Estado de Sao Paulo and University of Sao Paulo. This is Contribution No. NDRL-3617 from the Notre Dame Radiation Laboratory. The IR and Raman spectra were recorded by Professors Sandra Mutarelli and Paulo Sergio Santos at the Instituto de Quimica, Universidade de São Paulo, São Paulo, Brazil. The authors greatly appreciate their assistance with these measurements.

## References

1 L. Sacksteder, A. P. Zipp, E. A. Brown, J. Streich, J. N. Demas and B. A. Degraff, *Inorg. Chem.*, 1990, **29**, 4335.
2 T. A. Perkins, W. Humer, T. L. Netzel and K. S. Schanze, *J. Phys. Chem.*, 1990, **94**, 2229.
3 J. R. Shaw and R. H. Schmehl, *J. Am. Chem. Soc.*, 1991, **113**, 369.
4 M. M. Glezen and A. J. Lees, *J. Chem. Soc., Chem. Commun.*, 1987, 1952.
5 M. M. Glezen and A. J. Lees, *J. Am. Chem. Soc.*, 1988, **110**, 3892.
6 M. M. Glezen and A. J. Lees, *J. Am. Chem. Soc.*, 1988, **110**, 6243.
7 M. S. Wrighton and D. L. Morse, *J. Am. Chem. Soc.*, 1974, **96**, 998.
8 M. S. Wrighton, D. L. Morse and L. Pdungsap, *J. Am. Chem. Soc.*, 1975, **97**, 2073.
9 J. C. Luong, H. Faltynak and M. S. Wrighton, *J. Am. Chem. Soc.*, 1979, **101**, 1597.
10 P. J. Giordano, S. M. Fredericks, M. S. Wrighton and D. L. Morse, *J. Am. Chem. Soc.*, 1978, **100**, 2257.
11 J. C. Luong, L. Nadjo and M. S. Wrighton, *J. Am. Chem. Soc.*, 1978, **100**, 5791.
12 P. J. Giordano and M. S. Wrighton, *J. Am. Chem. Soc.*, 1979, **101**, 2888.
13 S. M. Fredericks, J. C. Luong and M. S. Wrighton, *J. Am. Chem. Soc.*, 1979, **101**, 7415.
14 D. P. Summers, J. C. Luong and M. S. Wrighton, *J. Am. Chem. Soc.*, 1981, **103**, 5238.
15 C. Shu and M. S. Wrighton, *Inorg. Chem.*, 1988, **27**, 4326.
16 J. Hawecker, J.-M. Lehn and R. Ziessel, *J. Chem. Soc., Chem. Commun.*, 1984, 328.
17 C. Kutal, M. A. Weber, G. Ferraudi and D. Geiger, *Organometallics*, 1985, **4**, 2161.
18 C. Kutal, A. J. Corbin and G. Ferraudi, *Organometallics*, 1987, **6**, 553.
19 M. Feliz and G. Ferraudi, *Chem. Phys. Lett.*, 1991, **181**, 201.
20 J. V. Caspar and T. J. Meyer, *J. Phys. Chem.*, 1983, **87**, 952.
21 P. Sullivan and T. J. Meyer, *J. Chem. Soc., Chem. Commun.*, 1984, 1244.
22 J. V. Caspar, B. P. Sullivan and T. J. Meyer, *Inorg. Chem.*, 1984, **23**, 2104.
23 T. D. Westmoreland, K. S. Schanze, P. E. Neveux, jun., E. Danielson, B. P. Sullivan, P. Chem and T. J. Meyer, *Inorg. Chem.*, 1985, **24**, 2597.
24 M. Feliz, G. Ferraudi and H. Altmiller, *J. Phys. Chem.*, 1992, **96**, 257.
25 M. Feliz and G. Ferraudi, *J. Phys. Chem.*, 1992, **96**, 3059.
26 D. J. Stufkens, *Comments Inorg. Chem.*, 1992, **13**, 359.
27 V. J. Koester, *Chem. Phys. Lett.*, 1975, **32**, 575.
28 S. Hotchandani and A. C. Testa, *J. Photochem. Photobiol. A: Chem.*, 1991, **55**, 323.
29 J. R. Huber, M. Mahaney and J. V. Morris, *Chem. Phys.*, 1976, **16**, 329.
30 Y. H. Li and E. C. Lim, *Chem. Phys. Lett.*, 1971, **9**, 279.
31 E. C. Lim and J. M. H. Yu, *J. Chem. Phys.*, 1967, **47**, 3270.
32 D. T. Cromer and J. T. Weber, in *International Tables for X-Ray Crystallography*, Kynoch Press, Birmingham, 1974, vol. 4, Table 2.2B.
33 J. A. Ibers and W. C. Hamilton, *Acta Crystallogr.*, 1964, **17**, 781.
34 D. T. Cromer, in *International Tables for X-Ray Crystallography*, Kynoch Press, Birmingham, 1974, vol. 4, Table 2.3.1.
35 W. J. Cruickshank, *Acta Crystallogr.*, 1949, **2**, 154.
36 B. A. Frenz, in *Computing in Crystallography*, eds. H. Schenk, R. Olthof-Hazelkamp, H. van Konigsveld and G. C. Bassi, Delft University Press, Delft, 1978, pp. 64–71.
37 B. Kraut and G. Ferraudi, *J. Chem. Soc., Dalton Trans.*, 1991, 2063 and refs. therein.
38 B. Kraut and G. Ferraudi, *Inorg. Chem.*, 1990, **29**, 4834.
39 B. Kraut and G. Ferraudi, *Inorg. Chem.*, 1989, **28**, 4578.
40 P. Chen, M. Curry and T. J. Meyer, *Inorg. Chem.*, 1989, **28**, 2271.
41 A. Streitwaiser, in *Molecular Orbital Theory for Organic Chemists*, Wiley, New York, 1961.
42 K. Nakamoto, in *Infrared and Raman Spectra of Inorganic and Coordination Compounds*, 3rd edn., Wiley, New York, 1978.
43 G. Ferraudi, in *Elements of Inorganic Photochemistry*, Wiley-Interscience, New York, 1988.
44 A. B. P. Lever, in *Inorganic Electronic Spectroscopy*, 2nd edn., Elsevier, New York, 1984.

*Received* 18*th January* 1994; *Paper* 4/00322E